Korean J. Chem. Eng., 19(2), 239-245 (2002)

Study of Polystyrene Degradation Using Continuous Distribution Kinetics in a Bubbling Reactor

Wang Seog Cha†, Sang Bum Kim* and Benjamin J. McCoy**

School of Civil and Environmental Engineering, Kunsan National University, Kunsan 573-701, Korea
*Department of Chemical Engineering, Korea University, Seoul 136-701, Korea
**Department of Chemical Engineering and Material Science, University of California, Davis, CA 95616, USA
(*Received 3 April 2001 • accepted 10 September 2001*)

Abstract–A bubbling reactor for pyrolysis of a polystyrene melt stirred by bubbles of flowing nitrogen gas at atmospheric pressure permits uniform-temperature distribution. Sweep-gas experiments at temperatures 340-370 °C allowed pyrolysis products to be collected separately as reactor residue(solidified polystyrene melt), condensed vapor, and uncondensed gas products. Molecular-weight distributions (MWDs) were determined by gel permeation chromatography that indicated random and chain scission. The mathematical model accounts for the mass transfer of vaporized products from the polymer melt to gas bubbles. The driving force for mass transfer is the interphase difference of MWDs based on equilibrium at the vapor-liquid interface. The activation energy and pre-exponential of chain scission were determined to be 49 kcal/mol and 8.94×10^{13} s^{-1}, respectively.

Key words: Pyrolysis, Molecular-Weight-Distribution, Random Scission, Chain-end Scission, Continuous Distribution Theory

INTRODUCTION

Fundamental and practical studies of plastics processing, such as energy recovery (production of fuel) and tertiary recycle (recovery of chemicals) [Carniti et al., 1991] are being promoted. Both of these recycling processes are based on chemical decomposition of polymers to low molecular-weight (MW) compounds. For process design, development, and evaluation, a complete quantitative description would entail mathematical modeling of the composition of the reaction mixture during thermolysis by accurate representation of decomposition rates.

The review [Westerout et al., 1997a] of low-temperature pyrolysis (T<450 °C) states that most chemical-reaction kinetics studies of pyrolysis were performed by standard thermogravimetric analysis (TGA). Weight-loss data for a small polymer mass (a several milligram sample) in a small heated crucible comprise the primary information for determining pyrolysis kinetics. The review, in a critical discussion of several models for analyzing TGA data, pointed out that the observed weight loss in pyrolysis involves evaporation of low-MW products. Any low-MW molecules in the polymer will initially evaporate. The empirical power-law rate expression employed in most studies to fit TGA weight-loss data is considered valid only at large polymer conversions, where random scission of the remaining low-MW polymer molecules yields volatile products. The widespread use of the simple power-law model is a probable reason that reported rate coefficients differ by a factor of 10. Reported kinetic parameters (pre-exponential factor and activation energy) for polymer also cover a wide range.

Westerout et al. proposed a random-chain dissociation (RCD) model, based on evaporation of depolymerization products less than a certain chain length. In a subsequent paper [Westerout et al., 1997b] on screen-heater pyrolysis, the RCD model was further described. For the screen-heated system, as well as for thermogravimetry, mass transfer of vaporized depolymerization products can strongly influence rate. Such interphase mass transfer depends on a driving force that should account for equilibrium at the vapor-liquid (melt) interface. Evaluation of a flow reactor with entrained polymer particles [Westerout et al., 1996] showed that melted particles tended to stick to the reactor walls, making their residence times unpredictable.

Seeger and Gritter [1997] studied pyrolysis of 1-mg samples of polyethylene and n-alkanes with programmed temperature rise under hydrogen sweep gas. Gas chromatographic analysis of the volatilized reaction products yielded a carbon-number distribution. Recognition of the key role of the volatilization process was the result of that work. Ng et al. [1995] used nitrogen as carrier gas for polyethylene pyrolysis and catalytic cracking, noting that volatile products were purged from the reactor and prevented from reacting.

For the most part, empirical reaction-kinetics expressions for weight loss due to volatilization of low-MW depolymerization products were applied in polymer pyrolysis studies. The mathematical models usually disregarded mass-transfer resistance for volatile depolymerization products. Understanding the chain-scission reactions that produce low-MW volatile products is obviously required for a fundamental quantitative description of pyrolysis. Many studies have tried to model random-chain scission, but chain-end scission, which is accompanied with random scission, has been ignored.

The present objective is to study pyrolysis and a mathematical model combining mass-transfer, interfacial vapor-liquid equilibrium, and chain-scission processes. We take experiments for a polystyrene melt decomposing at pyrolysis temperatures to form low-MW evaporating compounds. These products are swept away by flowing inert gas into a cooled flask where condensed vapors are trapped.

†To whom correspondence should be addressed.
E-mail: wscha@kunsan.ac.kr
‡Presented at the Int'l Symp. on Chem. Eng. (Cheju, Feb. 8-10, 2001), dedicated to Prof. H. S. Chun on the occasion of his retirement from Korea University.

The MWDs of reactor residue and liquid condensate are determined by HPLC gel permeation chromatography (GPC). Noncondensable gases are analyzed downstream by gas chromatography. Population balance equations, incorporating random and chain-end scission as well as liquid-vapor mass transfer, are applied to polymer melt, vapor, condensable vapor, and gas. An MW-moment method applied to the governing integrodifferential equations allows formulation of ordinary differential equations for zeroth moments (molar concentrations), first moments (mass concentrations), and second moments of melt, vapor, condensate, and gas MWDs.

EXPERIMENTAL

Polystyrene pyrolysis experiments were conducted at atmospheric pressure under nitrogen gas at 340, 350, 360 and 370 °C. The diagram of the experimental apparatus (Fig. 1) shows a polymer melt in the heated reactor (immersed in a molten-salt bath) and vapor carried to the condenser vessel (immersed in an ice bath) by flow of nitrogen sweep gas. The gas flows through 1.59 mm stainless steel tubing, 3.4 m of which is coiled and immersed in the molten salt so that the gas temperature reaches the bath temperature. Nitrogen enters at the reactor base through a 12.7 mm-diameter, 316 stainless steel frit (Supelco) with 2-μm pores, which disperse the gas but prevent backflow of the polymer melt. The stainless steel reactor of internal volume 10 cm^3 is fitted into a steel protective sleeve lined with a steel shot (3.4 mm diameter) to improve heat transfer. The volume available to condensable vapor, Vv=64 cm^3, includes reactor and condenser vapor spaces and a connecting tube. The volume available to noncondensable gas, Vg=324 cm^3, includes Vv and the tube leading away from the condenser.

The reactor holds 2 g of unreacted polystyrene pellets. The stainless steel tube leading from the reactor to the condenser vessel was wrapped with heating tape to maintain a temperature 5 °C higher than the reaction temperature. This prevented condensation in the line.

The cooled pyrolysis products at the end of an experiment are solid polymer remaining in the reactor, liquid condensate in the condenser vessel, and gas. Gas product was collected at 20-min intervals during the experiment and analyzed by GC. Reactor and condenser vessels were separately weighed before and after each experiment to determine the final polymer and condensate masses. Each product was dissolved at 25 °C in 100 ml of HPLC reagent-grade THF and analyzed by HPLC-GPC (Waters). Two GPC columns (Waters HR3) packed with cross-linked styrene-divinylbenzene copolymer beads (10-μm diameter) were used in series.

Conversion of MW from GPC retention time was computed by a spreadsheet computer program. Knowing the mass of the polymer and the volume of the solvent allows calculation of MWD as mass/MW. Mass MWDs are reported in this work as g/MW normalized for 1.00 g of initial sample (area under mass MWD represents 1.00 g). Molar MWDs can be calculated by dividing each mass MWD by MW. MW moments of these molar MWDs are represented as $P^{(n)}$ (the units are mol for n=0 and mass for n=1). The respective molar concentration moments are expressed on a volume basis, $p^{(n)}=P^{(n)}/V$.

The molecular weight distribution (Fig. 2) indicates a number average MW of 50,000 and a weight average MW of 210,000. The many peaks in the lower MW range would interfere with the analysis of the degradation products.

To eliminate these low MW peaks, the polymer was fractionated by partially dissolving 50 g of polymer in 500 ml of toluene. The solution was continuously stirred with a magnetic stirrer and 750 ml of

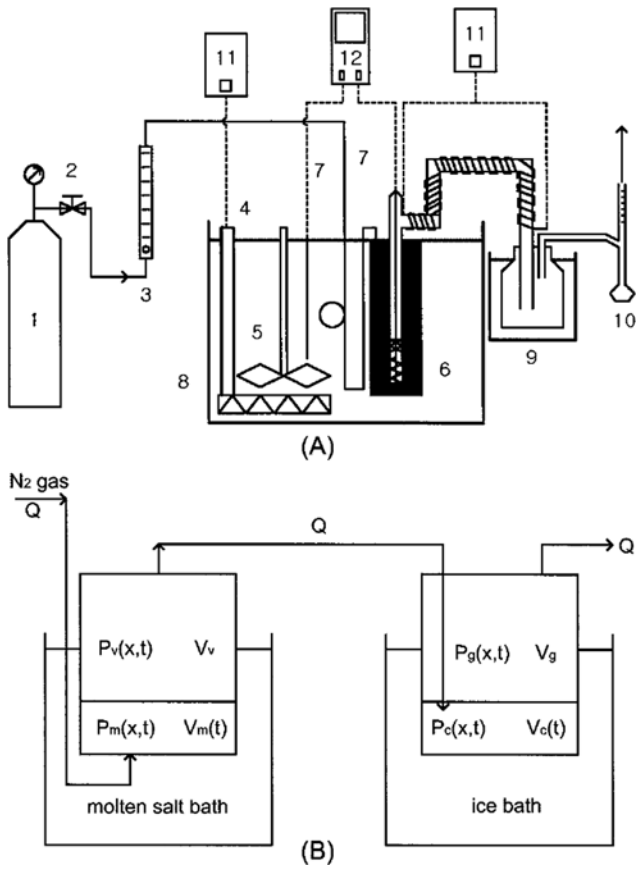

Fig. 1. (A) Schematic drawing of the experimental apparatus: (1) nitrogen cylinder, (2) valve, (3) rotameter, (4) heater, (5) stirrer, (6) reactor, (7) thermocouples, (8) molten-salt bath, (9) ice bath, (10) soap-bubble meter, (11) controllers, (12) digital thermometer readout. (B) Sketch of the apparatus for the mathematical model showing the notation for volumes, molar MWDs, and flow rate.

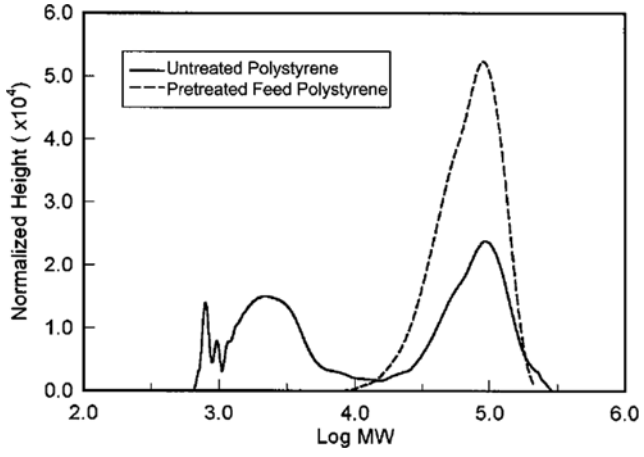

Fig. 2. Molecular weight distribution of untreated polystyrene and pretreated feed polystyrene.

the precipitating agent, 1-butanol, was slowly added until 70% of the polymer was precipitated. The precipitate was dried to a constant weight at 110 °C and stored under nitrogen. The molecular weight distribution of the treated polymer, with number average MW of 95,000 and weight average MW of 190,000, is shown in Fig. 2.

THEORY

The experimental apparatus (Fig. 1) shows a polymer melt in the heated reactor, vapor flow to the condenser vessel, and flow of inert nitrogen sweep gas. The subscripts m, v, c, and g denote polymer melt, condensable vapor, condensate, and noncondensable gas products, respectively. Polymer melt volume, V_m, decreases with reaction time due to evaporation of low-MW components. Condensate volume, V_c, increases with reaction time. Volume changes of the relatively large vapor volume, V_v, and gas-product volume, V_g, are negligible. The gas flow rate, Q, was constant.

MWDs [mol/(vol·MW)] are defined so that at time t, p(x, t) dx is the molar concentration (mol/volume) of a compound having values of MW x in the range x to x+dx. Moments of MWDs are defined as integrals over x,

$$p^{(n)}(t) = \int_0^\infty p(x,t)x^n dx \tag{1}$$

The zeroth moment (n=0) is the time-dependent total molar concentration (mol/volume). The first moment, $p^{(1)}(t)$, is the mass concentration (mass/volume). The normalized first moment (average MW) and second central moment (variance of the MWD) are given by $p^{avg}=p^{(1)}/p^{(0)}$ and $p^{var}=p^{(2)}/p^{(0)}-[p^{avg}]^2$, respectively. The polydispersity index is defined as the ratio of mass (or weight) average MW, $Mw=p^{(2)}/p^{(1)}$, to molar (or number) average MW, $Mn=p^{avg}$, thus, $D(\text{polydispersity})=p^{(2)}p^{(0)}/[p^{(1)}]^2$. The three moments, $p^{(0)}$, p^{avg}, and p^{var}, provide shape characteristics of the MWD and can be used to construct the MWD mathematically.

Population balances for the MWDs are based on mass balances; that is, the accumulation rate is equal to the net generation by reaction minus the net loss by flow or mass transfer. The mass-transfer rate from the polymer melt to vapor bubbles, described by an overall mass-trasfer coefficient, $k(x)=k_0-k_1x$, is assumed to decrease linearly with MW to account for lower mass-transfer rates of higher-MW components. The interphase mass-transfer driving force is given by p_m-p_v/K, where p_m, p_v, and K are all functions of x so that the driving force depends on the particular component that is evaporating. The vapor liquid phase equilibrium constant is assumed to decrease with MW according to an inverse polynomial

$$K(x) = K_0 \Big/ \left(1 + \sum_{j=1} a_j x^j\right) \tag{2}$$

These expressions for k(x) and K(x) permit mathematical solutions to the mass balance equations through MW moments.

Simultaneous random-scission and repolymerization reactions can be written as

$$P(x') \underset{k_a}{\overset{k_d}{\rightleftarrows}} P(x) + P(x'-x) \tag{A}$$

and irreversible chain-end scission as

$$P(x) \xrightarrow{k_s} Q(x_s) + P(x-x_s) \tag{B}$$

where $Q(x_s)$ is a monomer or oligomer of mass x_s. The rate expressions for reactions A and B have been related to radical mechanisms [Kodera and McCoy, 1997]. The random-scission rate should increase with the number of bonds that can be cleaved. Hence, k_d should generally increase with x [Madras et al., 1997].

Polymerization rates, according to the equal-reactivity approximation, are independent of MW. The chain-end scission rate is essentially proportional to the number of chain ends and is thus independent of the chain length and of x, the MW of a macromolecule [Wang et al., 1995]. The stoichiometric kernels and 1/x' for random scission and $\delta[x-(x'-x_s)]$ and $\delta(x-x_s)$ for the two products of chain-end scission. Rate expressions for reactions A and B have been applied previously in polymer degradation studies [Madras et al., 1996; Song and Hyun, 1999].

We consider that random-scission and repolymerization reactions, as well as chain-end scission, occur in the polymer melt with rate coefficients $k_d(x)$, k_a, and k_s, respectively. The random-scission rate coefficient is considered a function of x, whereas the two other coefficients are independent of x. The vapor is dilute as it is swept out of the reactor. Hence, no significant reaction occurs in the vapor. If composition is assumed uniform at any time throughout the gas bubbles and the liquid, the mass balances are as follows:

for *polymer melt*

$$\begin{aligned}\frac{\partial(V_m p_m)}{\partial t} = &-\chi(p_m - p_v/K) + V_m[-k_d(x)p_m(x) \\ &+ 2\int_x^\infty k_d(x')p_m(x')(1/x')dx' - 2k_a p_m(x)p_m^{(0)} \\ &+ k_a\int_0^\infty p_m(x')p_m(x-x')dx' - k_s p_m(x) \\ &+ k_s\int_x^\infty p_m(x')\delta[x-(x'-x_s)]dx']\end{aligned} \tag{3}$$

for *vapor*

$$\partial(V_v p_v)/\partial t = \chi(p_m - p_v/K) - Qp_v \tag{4}$$

for *condensate*

$$\partial(V_c p_c)/\partial t = Qp_v \tag{5}$$

for *noncondensable gas products*

$$\partial(V_g p_g)/\partial t = V_m k_s \int_x^\infty p_m(x')\delta(x-x_s)dx' - Qp_g \tag{6}$$

We first consider that k_d is constant with x and comment later on the effect of a linear dependence on x. Applying the moment operation to each equation yields [McCoy and Madras, 1997] the following differential equations:

for *polymer melt*

$$\begin{aligned}\frac{d(V_m p_m^{(n)})}{dt} = &-\chi_0\left[p_m^{(n)} - \left(p_v^{(n)} + \sum_{j=1} a_j p_v^{(n+j)}\right)/K_0\right] \\ &+\chi_1\left[p_m^{(n+1)} - \left(p_v^{(n+1)} + \sum_{j=1} a_j p_v^{(n+1+j)}\right)/K_0\right] \\ &+V_m[-k_d p_m^{(n)}(n-1)/(n+1) - 2k_a p_m^{(n)}p_m^{(0)} \\ &+k_a\sum_{j=0}^{n}(n_j)p_m^{(j)}p_m^{(n-j)} - k_s p_m^{(n)} + k_s\sum_{j=0}^{n}(n_j)(-x_s)^j p_m^{(n-j)}\Big]\end{aligned} \tag{7}$$

for *vapor*

$$\frac{d(V_v p_v^{(n)})}{dt} = +\chi_0\left[p_m^n - \left(p_v^n + \sum_{j=1} a_j p_v^{n+j}\right)/K_0\right] - \chi_1\left[p_m^{(n+1)} - \left(p_v^{(n+1)} + \sum_{j=1} a_j p_v^{(n+1+j)}\right)/K_0\right] - Qp_v^{(n)} \quad (8)$$

for *condensate*

$$d(V_c p_c^{(n)})/dt = Qp_v^{(n)} \quad (9)$$

for *noncondensable gas products*

$$d(V_g p_g^{(n)})/dt = V_m k_s x_s^n p_m^{(0)} - Qp_g^{(n)} \quad (10)$$

For n=0 the differential equations are molar balances:

for *polymer melt*

$$\frac{d(V_m p_m^{(n)})}{dt} = -\chi_0\left[p_m^{(0)} - \left(p_v^{(0)} + \sum_{j=1} a_j p_v^{(j)}\right)/K_0\right] + \chi_1\left[p_m^{(1)} - \left(p_v^{(1)} + \sum_{j=1} a_j p_v^{(j+1)}\right)/K_0\right] + V_m[k_d - k_a p_m^{(0)}]p_m^{(0)} \quad (11)$$

for *vapor*

$$\frac{d(V_v p_v^{(0)})}{dt} = +\chi_0\left[p_m^{(0)} - \left(p_v^{(0)} + \sum_{j=1} a_j p_v^{(j)}\right)/K_0\right] - \chi_1\left[p_m^{(1)} - \left(p_v^{(1)} + \sum_{j=1} a_j p_v^{(j+1)}\right)/K_0\right] - Qp_v^{(0)} \quad (12)$$

for *condensate*

$$d(V_c p_c^{(0)})/dt = Qp_v^{(0)} \quad (13)$$

for *noncondensable gas products*

$$d(V_g p_g^{(0)})/dt = V_m k_s x_s p_m^{(0)} - Qp_g^{(0)} \quad (14)$$

For n=1 the differential equations are mass balances:

for *polymer melt*

$$\frac{d(V_m p_m^{(1)})}{dt} = -\chi_0\left[p_m^{(1)} - \left(p_v^{(1)} + \sum_{j=1} a_j p_v^{(j+1)}\right)/K_0\right] + \chi_1\left[p_m^{(2)} - \left(p_v^{(2)} + \sum_{j=1} a_j p_v^{(j+2)}\right)/K_0\right] - V_m k_s x_s p_m^{(0)} \quad (15)$$

for *vapor*

$$\frac{d(V_v p_v^{(1)})}{dt} = +\chi_0\left[p_m^{(1)} - \left(p_v^{(1)} + \sum_{j=1} a_j p_v^{(j+1)}\right)/K_0\right] - \chi_1\left[p_m^{(2)} - \left(p_v^{(2)} + \sum_{j=1} a_j p_v^{(j+2)}\right)/K_0\right] - Qp_v^{(1)} \quad (16)$$

for *condensate*

$$d(V_c p_c^{(1)})/dt = Qp_v^{(1)} \quad (17)$$

for *noncondensable gas products*

$$d(V_g p_g^{(1)})/dt = V_m k_s x_s p_m^{(0)} - Qp_g^{(1)} \quad (18)$$

If these four mass balance equations are added, terms cancel so that the rate of change of the total mass, $m_{tot}=P_m^{(1)}+P_v^{(1)}+P_c^{(1)}+P_g^{(1)}$, equals the loss of gas products in the outflow,

$$dm_{tot}/dt = -QP_g^{(1)} \quad (19)$$

thus recovering the overall mass balance for the equipment. Because $dP_g^{(1)}/dt$ is vanishingly small, from Eq. (18) and the definition of the polymer melt MW, M_{nm}, we have

$$dm_{tot}/dt = -k_s(x_s/M_{nm})P_m^{(1)} \quad (20)$$

According to this equation, the rate of change of the total polymer mass is first-order in melt mass, $P_m^{(1)}=V_m p_m^{(1)}$. This is a rationale for the first-order rate expression that is frequently applied to calculate rate coefficients for pyrolysis data [Westerout et al., 1997]. The calculation, however, is usually based on polymer melt mass, $P_m^{(1)}$, rather than total mass, m_{tot}, according to the supposed first-order expression

$$dP_m^{(1)}/dt \approx -k_{s,appr}P_m^{(1)} \quad (21)$$

Eq. (21) ignores the vaporization contribution to weight loss and lumps all chain-scission processes into one rate constant. Therefore, this expression is an approximation to the realistic rate.

Initial conditions for polymer melt and condensate MWDs are $p_m(x, 0)$ and $p_c(x, 0)$ and, for moments, $p_m^{(0)}(0)$ and $p_c^{(0)}(0)$.

RESULTS AND DISCUSSION

Experimental results demonstrate how MWDs of reactor poly-

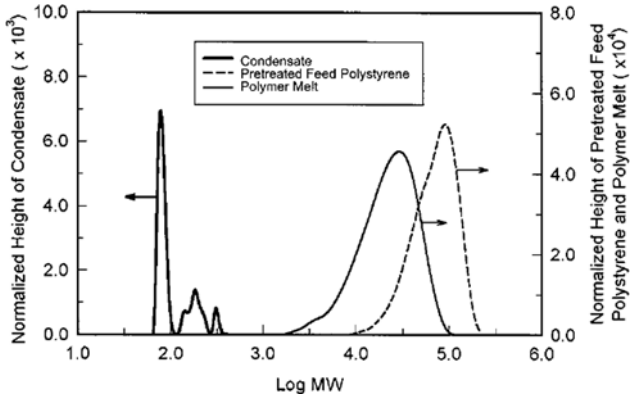

Fig. 3. Molecular weight distribution of pretreated feed polystyrene, polymer melt and condensate (pyrolysis temperature: 360 °C, pyrolysis time: 1 hr).

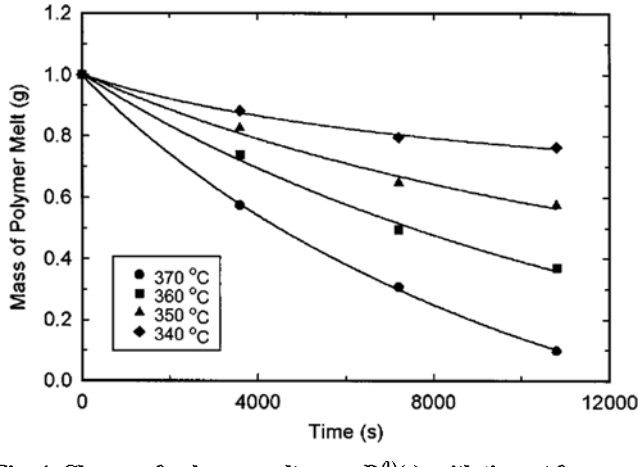

Fig. 4. Change of polymer melt mass, $P_m^{(1)}$(g), with time at four pyrolysis temperatures.

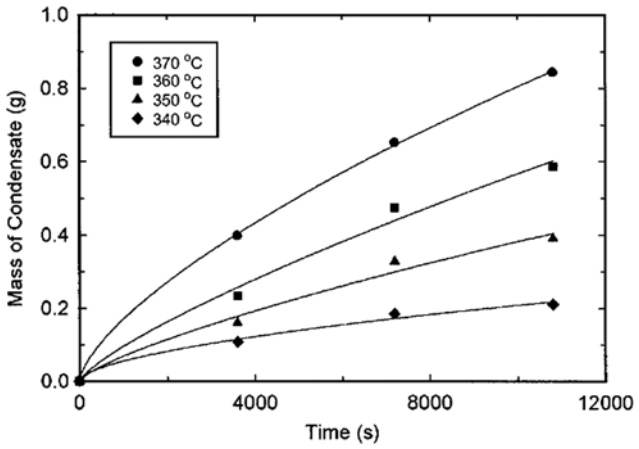

Fig. 5. Change of condensate mass, $P_c^{(1)}$(g), with time at four pyrolysis temperatures.

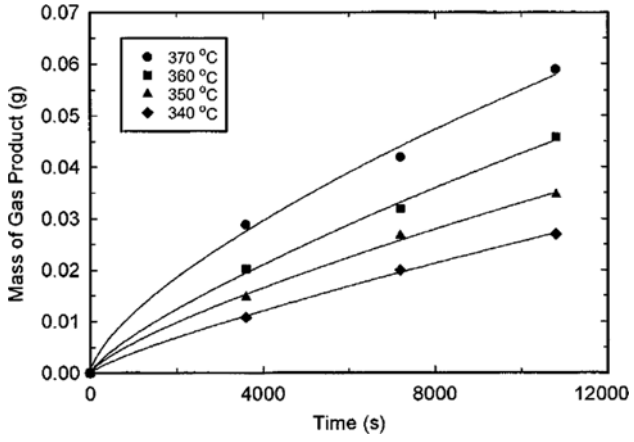

Fig. 7. Change of cumulative gas product mass, N_g(g), with time at four pyrolysis temperatures.

mer and vaporized depolymerization products vary with time.

Fig. 3 represents the molecular weight distribution of pretreated feed polystyrene and its degradation products. Polymer remaining in the reactor after pyrolysis time is mainly produced by random scission and condensate collected in the condensate vessel is produced by the chain end scission.

Typical pyrolysis experiments measure only loss of polymer mass due to evaporation of depolymerization products and unreacted low-MW polymer. The present approach provides two measurements of reactor polymer mass (Fig. 4) and of condensate (Fig. 5) at the end of each experiment. One method of the measurements is by weighing and the other is by the first moment of the MWD, which requires that the weight be known. As the measurements are not independent, reactor polymer mass and condensate mass calculated by the two methods coincide. Reactor polymer mass decreases with increasing the condensate, and their sum decreases with time due to gas product loss (Fig. 6). The mass of gaseous products (Fig. 7) is found by subtracting the sum of polymer melt and condensate masses from the initial polymer mass. For example, at 370 °C and 3 h, 10% of the original polymer remains in the reactor while 84% is condensate and 6% gaseous products. As temperature and time increase, the reactor polymer mass decrease while condensate and gas-product masses increase. The time dependences of polymer-melt mass, condensate mass, combined mass, and product-gas mass were approximated as second-order polynomials (Figs. 4-7).

The condensate accumulation rate increases with the gas flow rate, as indicated by Eqs. (5), (9), (13), and (17). Higher flow rates cause the mass of the reactor melt to be smaller and the mass of the condensate to be larger. The influence of flow rate is greater at higher temperatures and longer reaction times. As the reaction temperature approaches the boiling point of the polymer melt, vaporization increases.

The moles of reactor polymer, $P_m^{(0)}$, decrease with time (Fig. 8), because low-MW products are vaporized. Chain-end scission to produce gas products and very low-MW liquid products does not change the polymer molar concentration.

The moles of condensate, $P_c^{(0)}$, increase with time (Fig. 9) due to accumulation of condensed vapor. Calculations by Eq. (13) show the vapor molar concentration is only 2% of the polymer melt molar concentration, which confirms the negligible contribution of vapor degradation.

Following application of the moment operation, mass-transfer terms cancel when melt and condensate moment equations are added. Thus, numerical values of coefficients in the mass-transfer polynomial values expressions will not directly affect final results or con-

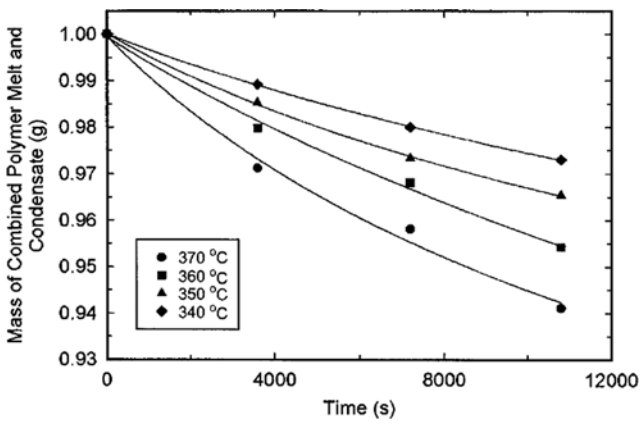

Fig. 6. Change of combined polymer melt and condensate masses, $P_m^{(1)}+P_c^{(1)}$(g), with time at four pyrolysis temperatures.

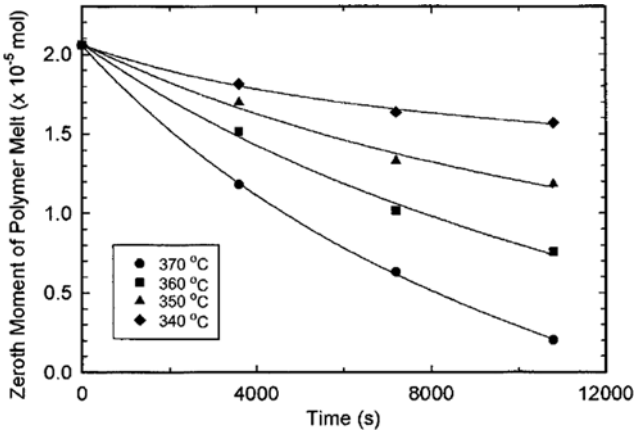

Fig. 8. Change of the zeroth moment, $P_m^{(0)}$(mol), of the polymer melt with time at four pyrolysis temperatures.

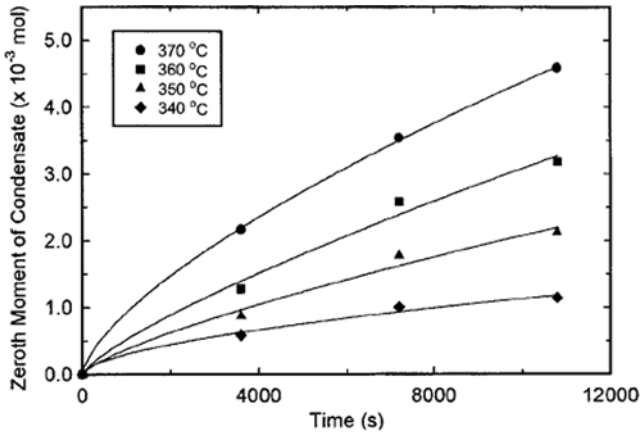

Fig. 9. Change of the zeroth moment, $P_c^{(0)}$(mol), of the condensate with time at four pyrolysis temperatures.

clusions. Relative amounts of reactor residue and condensate, however, do depend on the mass-transfer rate and therefore on the sweep-gas flow rate.

Density of the polystyrene was determined by heating 1.00 g of raw polystyrene in a tube and measuring the volume in the temperature range 151-295 °C. The weight of the tube and contents did not change, indicating there are no vaporization losses in this temperature range. The density (g/cm^3) as a function of temperature (°C) was fitted with a 2nd degree polynomial,

$$P_m = 0.996 - 0.0015T + 2\times10^{-6}\,T^2 \qquad (22)$$

and extrapolated to 370 °C to calculate polymer-melt volume from melt mass.

After an experiment, weights of reactor residue and condensate were determined by weighing reactor and condensate vessels with their contents and subtracting weights of the empty vessels. Polymer-melt volume as a function of time, $V_m(t)$, was determined from reactor residue mass (Fig. 4) and density (Eq. (22)). Values of V_m versus time at four reaction temperatures (Fig. 10) are well approximated. The condensate volume, $V_c(t)$, was calculated from condensate mass (Fig. 5) and density, measured as 0.79 g/cm^3. Values of V_c versus time at four reaction temperatures (Fig. 11) are fitted

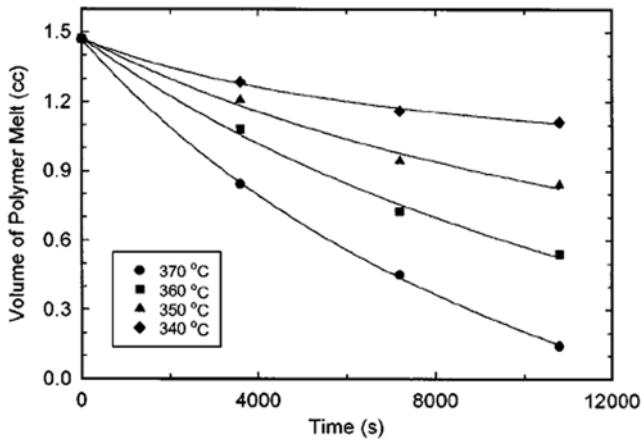

Fig. 10. Change of the polymer melt volume, V_m(cc), with time at four pyrolysis temperatures.

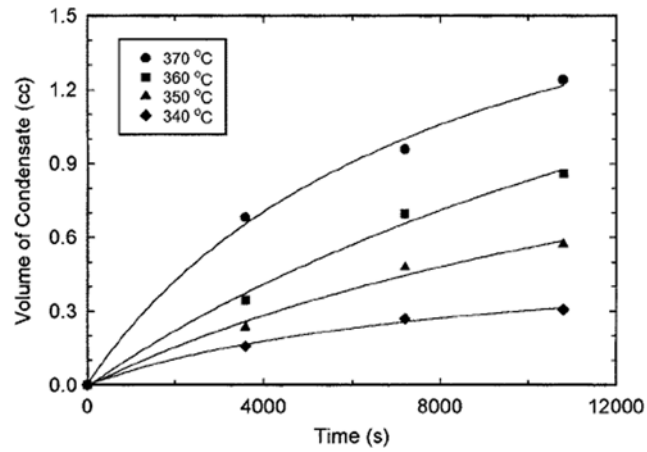

Fig. 11. Change of condensate volume, V_c(cc), with time at four pyrolysis temperatures.

with 2nd-order polynomials.

An approximate estimate of the chain scission rate coefficient can be determined from the mass of the polymer melt, $P_m^{(1)}$. By applying Eq. (21), we calculated an approximate rate coefficient, $k_{s,ap}$,

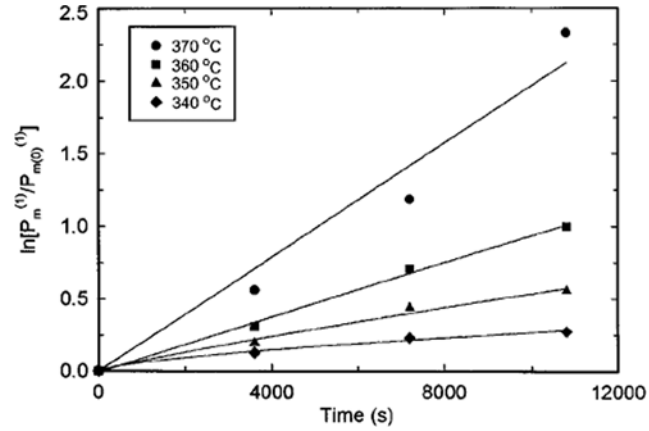

Fig. 12. Plot of $\ln[P_m^{(1)}/P_{m(0)}^{(1)}]$ versus time at four pyrolysis temperatures.

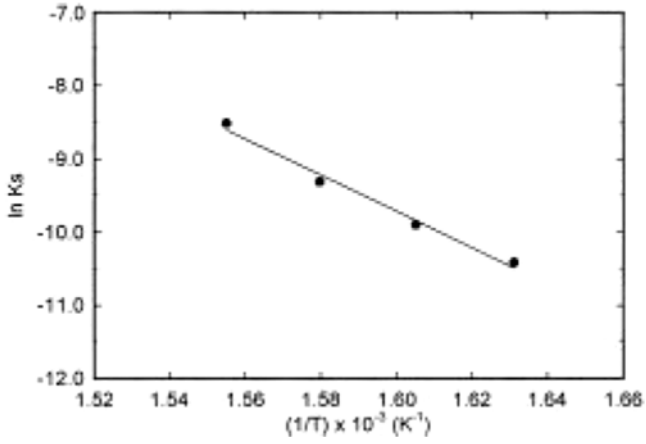

Fig. 13. Arrhenius plot for a polystyrene chain scission rate coefficient.

at each reaction temperature from the slope of $\ln[P_m^{(1)}(t)/P_m^{(1)}(0)]$ versus time (Fig. 12). The Arrhenius plot of these rate coefficients gave the activation energy of 49 kcal/mol and prefactor 8.94×10^{12} s^{-1} (Fig. 13). Compared with other reports, these values are similar to recommended values. For example, Westerhout et al. [1997a] for polystyrene suggested 49 kcal/mol and 10^{13} s^{-1}, and Kim et al. [1999] also suggested 53 kcal/mol for polystyrene of MW 222,000.

CONCLUSIONS

The analysis and results of this investigation are for a two-phase, plastics-pyrolysis process with polymer degradation occurring in the polymer melt. Lower-MW products formed by random scission volatilize by mass transfer and are condensed downstream. The driving force for mass transfer depends on the vapor-liquid equilibrium, for which volatility decreases with increasing MW. Capturing and analyzing the condensable vapors separately from the reactor polymer facilitates the analysis and interpretation of reaction data. The MWDs of polymer and condensate, determined by HPLC-GPC, permit important features of the physical and chemical reaction processes to be better understood and interpreted. The mathematical model applied to the experimental data was based on distribution kinetics, by which population-balance equations for MWDs are formulated as mass balances. These integrodifferential equations for melt, vapor, condensate, and gas were converted to ordinary differential equations by an MW-moment method. The resulting set of equations could be used to interpret the experimental data. The chain scission rate coefficient, $k_s=As\exp(-E_s/RT)$, was computed from data at different temperatures, yielding E_s=49 kcal/mol and $As=8.94\times10^{13}$ s^{-1} for polystyrene.

NOMENCLATURE

As	: pre-exponential factor [s^{-1}]
Es	: activation energy [kcal/mole]
k	: mass transfer coefficient [m/s]
K	: equilibrium constant
k_s	: rate coefficient [s^{-1}]
m_{tot}	: total mass [kg]
$p_c^{(0)}$	: zeroth moment of condensate [mole/m^3]
$P_c^{(0)}$	: moles of condensate [mole]
$p_c^{(1)}$	: first moment of condensate [kg/m^3]
$P_c^{(1)}$	: mass of condensate [kg]
$p_g^{(0)}$	: zeroth moment of gas product [mole/m^3]
$P_g^{(0)}$	: moles of gas product [mole]
$p_g^{(1)}$	: first moment of gas product [kg/m^3]
$P_g^{(1)}$	: mass of gas product [kg]
$p_m^{(0)}$	: zeroth moment of polymer melt [mole/m^3]
$P_m^{(0)}$	: moles of polymer melt [mole]
$p_m^{(1)}$	: first moment of polymer melt [kg/m^3]
$P_m^{(1)}$	: mass of polymer melt [kg]
P(x, t)	: molar concentration of a compound having values of MW x at time t [mole/m^3]
Q	: gas flow rate [m^3/s]
t	: time [s]
V_c	: volume of polymer melt [m^3]
V_g	: volume of gas product [m^3]
V_m	: volume of polymer melt [m^3]
V_v	: volume of vapor volume [m^3]

REFERENCES

Carniti, P., Beltrame, P. L., Massimo, A., Gervasini, A. and Audisio, A., "Polystyrene Thermodegradation. 2. Kinetics of Formation of Vloatile Products," *Ind. Eng. Chem. Res.*, **30**, 1624 (1991).

Kim, Y. S., Hwang, G. C., Bae, S. Y., Yi, S. C., Moon, S. K. and Kumazawa, H., "Pyrolysis of Polystyrene in a Batch-Type Stirred Vessel," *Korean J. Chem. Eng.*, **16**, 161 (1999).

Kodera, Y. and McCoy, B. J., "Continuous-Distributions Kinetics of Radical Mechanisms for Polymer Decomposition and Repolymerization," *AIChE J.*, **43**, 3205 (1997).

Madras, G., Smith, J. M. and McCoy, B. J., "Degradation of Poly(methyl methacrylate) in Solution," *Ind. Eng. Chem. Res.*, **35**, 1795 (1996a).

Madras, G., Smith, J. M. and McCoy, B. J., "Degradation of Poly(α-methylstyrene) in Solution," *Polym. Degrad. Stab.*, **52**, 349 (1996b).

Madras, G., Chung, G. Y., Smith, J. M. and McCoy, B. J., "Molecular Weight Effect on the Dynamics of Polystylene Degradation," *Ind. Eng. Chem. Res.*, **36**, 2019 (1997).

McCoy, B. J. and Madras, G., "Degradation Kinetics of Polymer in Solution: Dynamics of Molecular Weight Distributions," *AIChE J.*, **43**, 802 (1997).

Ng, S. H., Seoul, H., Stanciulescu, M. and Sugimoto, Y., "Conversion of Polyethylene to Transportation Fuels through Pyrolysis and Catalytic Cracking," *Energy Fuels*, **9**, 735 (1995).

Seeger, M. and Gritter, R. J., "Thermal Decomposition and Volatilization of Poly(α-olefins)," *J. Polym. Sci.*, **15**, 1393 (1977).

Song, H. and Hyun, J. C., "An Optimization Study on the Pyrolysis of Polystyrene in a Batch Reactor," *Korean J. Chem. Eng.*, **16**, 316 (1999).

Wang, M., Smith, J. M. and McCoy, B. J., "Continuous Kinetics for Thermal Degradation of Polymer in Solution," *AIChE J.*, **41**, 1521 (1995).

Westerhout, R. W. J., Kuipers, J. A. M. and Van Swaaij, W. P. M., "Development, Modelling and Evaluation of a (Laminar) Entrained Flow Reactor for the Determination of the Pyrolysis Kinetics of Polymer," *Chem. Eng. Sci.*, **51**, 2221 (1996).

Westerhout, R. W. J., Waanders, J., Kuipers, J. A. M. and Van Swaaij, W. P. M., "Kinetics of the Low Temperature Pyrolysis of Polyethene, Polypropene, and Polystyrene Modeling, Experimental Determination, and Comparison with Literature Models and Data," *Ind. Eng. Chem. Res.*, **36**, 1955 (1997a).

Westerhout, R. W. J., Balk, R. H. P., Meijer, R., Kuipers, J. A. M. and Van Swaaij, W. P. M., "Examination and Evaluation of the Use of Screen Heater for the Measurement of the High-Temperature Pyrolysis Kinetics of Polyethene and Polypropene," *Ind. Eng. Chem. Res.*, **36**, 3360 (1997b).